

NASA TN D-3989

NASA TECHNICAL NOTE



NASA TN D-3989

FACILITY FORM 602

N67-26549	
(ACCESSION NUMBER)	(THRU)
26	1
(PAGES)	(CODE)
	24
(NASA CR OR TMX OR AD NUMBER)	(CATEGORY)

PROTON BOMBARDMENT OF HIGH-PURITY SINGLE-CRYSTAL SILICON

by J. B. Robertson, R. K. Franks,

Langley Research Center

Langley Station, Hampton, Va.

and T. E. Gilmer, Jr.

Virginia Polytechnic Institute

Blacksburg, Va.

GPO PRICE \$ _____

CFSTI PRICE(S) \$ 3.00

Hard copy (HC) _____

Microfiche (MF) .65

ff 653 July 65

PROTON BOMBARDMENT OF HIGH-PURITY SINGLE-CRYSTAL SILICON

By J. B. Robertson, R. K. Franks,

Langley Research Center
Langley Station, Hampton, Va.

and T. E. Gilmer, Jr.

Virginia Polytechnic Institute
Blacksburg, Va.

NATIONAL AERONAUTICS AND SPACE ADMINISTRATION

For sale by the Clearinghouse for Federal Scientific and Technical Information
Springfield, Virginia 22151 - CFSTI price \$3.00

PROTON BOMBARDMENT OF HIGH-PURITY SINGLE-CRYSTAL SILICON¹

By J. B. Robertson, R. K. Franks,
Langley Research Center

and T. E. Gilmer, Jr.
Virginia Polytechnic Institute

SUMMARY

Bombardment of high-purity silicon with 22-MeV protons has produced Al²⁷ at a rate of 6×10^{-3} atom per proton in a thick target. The aluminum was identified by the Al_s infrared absorption spectrum. The production of aluminum in the crystals eliminated the study of damage in impurity-free silicon but, in return, provided for a study of defect interactions with aluminum. The production rate of aluminum is high enough that anyone studying radiation damage by protons should be aware of the presence of the aluminum.

Three new infrared absorption bands were observed in the irradiated silicon with main peaks at 8.9, 14.2, and 21.0 microns. Production of the 21.0-micron band required high sample temperature during bombardment and is identified as (substitutional aluminum) + (vacancy cluster). The 8.9- and 14.2-micron peaks appear and disappear with successive annealing. The possibility is mentioned that one or both of these lines might be due to $(\text{Al}_{\text{substitutional}}^- + \text{Al}_{\text{interstitial}}^{++})^+$. The 20.5-micron absorption band, which has been reported in neutron irradiated silicon, was found in proton irradiated silicon.

INTRODUCTION

Radiation damage to solids has been of interest ever since the development of the nuclear reactor. An increased interest has risen with the exploration of space because of the radiation fluxes encountered by spacecraft in their orbits. Radiation damage in semiconductors is studied by those whose primary interest is in radiation damage and who use semiconductors as tools in the study of the basic damage process in solids. The usefulness of semiconductors in this way is due to the fact that their measurable electrical and optical properties are greatly dependent upon crystal imperfections and impurities and are therefore very sensitive to radiation damage. Radiation damage in semiconductors is also studied by those whose primary interest is in semiconductors and who use radiation to introduce imperfections and energy levels into the crystals. It is also studied because

¹The essential material in this report was submitted by James B. Robertson as a dissertation in partial fulfillment of the requirements for the degree of Doctor of Philosophy in Physics at Virginia Polytechnic Institute, Blacksburg, Va., May 1966.

of the practical applications of semiconductors as particle detectors in radiation fields and as transistors, rectifiers, and solar cells in spacecraft.

The bulk of the work thus far has been done with doped semiconductors, mainly because the usefulness of semiconductors is derived from the effects of the chemical impurities. There have been, however, several reported results (refs. 1 to 6) which indicate that the effect of radiation on a semiconductor is dependent upon the types and amounts of chemical impurities present in the crystal.

This paper reports research on the proton bombardment of high-purity single-crystal silicon. High-purity silicon was used for this study in an attempt to assess the effects of chemical impurities in the damage process. The silicon crystals were bombarded with 22-MeV protons from a cyclotron; and the resulting damage was studied by infrared absorption and resistivity measurements.

REVIEW OF LITERATURE

The first serious study of radiation damage in semiconductors was done by Karl Lark-Horovitz and coworkers in 1947 (ref. 7) when they subjected germanium to reactor neutrons. Since then, the study has spread to other elemental and compound semiconductors, and the types of radiation now include photons, electrons, protons, neutrons, and heavier particles. The methods of study have also grown numerous: measurements of resistivity, excess carrier lifetime, carrier removal rate, infrared absorption, photoconductivity, Hall coefficient, and electron spin resonance.

In the theoretical consideration of damage to a perfect crystal of pure silicon by low-energy particles, the effects are limited to the production of vacancies, interstitials, and combinations thereof. The vacancies are lattice sites without a silicon atom; interstitials are the displaced atoms (a silicon atom between lattice sites); and combinations thereof include close vacancy-interstitial pairs (Frenkel defects), divacancies, etc. In practice, however, the silicon crystals contain lattice defects and many chemical impurities, and the incident particles may be of high energy. This condition adds impurity-damage associations, nuclear transmutations, and disordered regions to the results that are possible.

The most readily detected effect of radiation on a semiconductor is the change in the electrical properties caused by the production of energy levels within the forbidden energy gap. In the study of radiation damage in semiconductors, therefore, the emphasis is placed on the study of these energy levels. This work includes the study of the production, elimination, and change in charge state of the energy levels, as well as a determination of their position in the band gap, and the identification or proposal of a model of the defect responsible for the level.

Energy levels in the band gap of irradiated silicon have been reported by several workers. Wertheim (refs. 8 and 9) used electrons for bombardment and measured the conductivity, carrier lifetime, and Hall coefficient. Spitzer and Fan (ref. 10) and Ramdas and Fan (ref. 11) used neutron and electron bombardment and studied the damage with infrared absorption. Bemski (ref. 12) and Watkins and Corbett (ref. 13) used electron bombardment and electron spin resonance studies. Table 1 is a list of reported energy levels (refs. 9 and 14 to 19) in the band gap of irradiated silicon. The types of radiation and techniques used to determine the position of the energy level are included.

TABLE 1.- ENERGY LEVELS IN IRRADIATED SILICON

Position in band gap ¹	Type of irradiation	Method of detection	References
$E_C - 0.03$ eV	Electrons	Hall and resistivity	15
$E_C - 0.16$ eV	Electrons	Hall and resistivity	9, 16
$E_C - 0.16$ eV	Neutrons	Infrared absorption	14
$E_C - 0.17$ eV	Electrons	Hall and resistivity	15
$E_C - 0.17$ eV	Protons	Hall and resistivity	17
$E_C - 0.21$ eV	Neutrons	Infrared absorption	14
$E_C - 0.40$ eV	Electrons	Hall and resistivity	15, 16
$E_C - 0.40$ eV	Protons	Hall and resistivity	17
$E_V + 0.36$ eV	Electrons	Hall and resistivity	16
$E_V + 0.30$ eV	Electrons	Hall and resistivity	15
$E_V + 0.30$ eV	Neutrons	Hall and resistivity	18
$E_V + 0.29$ eV	Protons	Hall and resistivity	17
$E_V + 0.268$ eV	Electrons	Hall and resistivity	9
$E_V + 0.25$ eV	Neutrons	Infrared absorption	14
$E_V + 0.16$ eV	Neutrons	Hall and resistivity	18
$E_V + 0.15$ eV	Electrons	Hall and resistivity	16
$E_V + 0.055$ eV	Deuterons	Hall and resistivity	19
$E_V + 0.05$ eV	Electrons	Hall and resistivity	15

¹ E_C is defined as conduction band minimum; E_V is defined as valence band maximum.

Measurement of the optical absorption in silicon has proven to be an important method of studying radiation defects. It gives a direct measure of the energy of electronic transitions and of the concentration of the defects. It detects the ionization of donors and acceptors, which can be detected by electrical measurements, and also detects bound state excitations and atomic vibrations which do not affect the electrical properties. A disadvantage of optical absorption is the larger concentrations of defects required. Optical studies of irradiated semiconductors were first reported in 1952 by Becker et al. (ref. 20) who noted an absorption band at 1.8μ and a shift of the intrinsic

absorption edge in irradiated silicon. Since then, other optical studies have been reported (refs. 10, 11, 14, 22, and 23). Table 2 gives the wavelengths of reported absorption bands in irradiated silicon along with the type of bombarding particle and distinguishing characteristics of the silicon samples.

TABLE 2.- REPORTED ABSORPTIONS IN IRRADIATED SILICON

Wavelength, μ	Type of irradiation	Distinguishing characteristics of silicon	References
1.8	Electrons	n, p-type	22
1.8	Protons	n, p-type	(a)
1.8	Neutrons	p-type	14
3.6	Electrons	n, p-type	22, (b)
3.6	Protons	n, p-type	(a)
3.6	Neutrons	n-type	14
3.9	Neutrons	p-type	14
5.5	Neutrons	n-type	14
6.0	Electrons	Not specified	(b)
6.0	Neutrons	p-type	14
8.0	Electrons	Not specified	(b)
12.0	Electrons	Oxygen-rich	21, 22, (b)
12.0	Protons	Oxygen-rich	(a)
12.0	Neutrons	Oxygen-rich	11
20.5	Neutrons	n, p-type	14

^aUnpublished Langley data.

^bAbsorptions reported by RCA Laboratories (Princeton)
under NASA Contract NAS 5-457 (Third Semiannual Report).

Two theories for the energy levels of primary defects in semiconductors have been proposed. Both theories present models to predict the energy levels associated with simple isolated vacancies and isolated interstitials in a perfect silicon or germanium lattice. The JLH model proposed by James and Lark-Horovitz (ref. 7) in 1951 attributes two donor levels to each interstitial atom and two acceptor levels to each vacancy. A later model proposed by Blount (ref. 23) allows each type of defect to act as either a donor or an acceptor.

An excellent example of a physical model built from experimental evidence is the "Si-A center" (ref. 13). The Si-A center is identified as an oxygen atom which has trapped a mobile vacancy and is bridging two of the four broken bonds of the vacancy. It is responsible for an energy level 0.17 eV below the conduction band edge, $E_C - 0.17$ eV, an absorption band at 12 microns, and the "Si-A" electron spin resonance.

There is experimental evidence (refs. 1 to 6) which implies that chemical impurities play a major role in the production and existence of radiation defects in semiconductors.

Also, mounting evidence reported in references 2, 5, 12, and 24 indicates that the isolated vacancies and interstitials produced by irradiation in silicon do not remain in the crystal at room temperature and perhaps do not remain even at liquid-nitrogen temperature. Lifetime and resistivity measurements on irradiated silicon show annealing of the defects at 80° K (ref. 5). Results of electron paramagnetic resonance (EPR) studies on silicon irradiated at 4° K are interpreted as vacancy motion at 60° K and interstitial motion at 4° K (ref. 24).

The amount of work done to date in which protons are used for irradiation is relatively small. Most of the irradiation work has been done by use of electrons and neutrons, mainly because high energy electron and neutron sources are more readily available. Also, electron bombardment is used when the damage is to be limited to primary defects. Protons were used as the bombarding particles in the present investigation, oddly enough, because of their availability and because of the need for high concentration of defects for the infrared studies.

Carter and Downing (ref. 17) have bombarded silicon with 10-MeV, 26-MeV, and 40-MeV protons and measured the temperature dependence of the Hall coefficient and Hall mobility. The defect energy levels which they found in the proton-irradiated silicon have also been found in electron- and neutron-irradiated silicon. The same authors have made similar studies of electron-irradiated silicon and report that the introduction rate of defects is about 100 times greater for protons than for electrons. G. F. Hill of Langley Research Center has measured infrared absorption in proton-irradiated silicon (unpublished). The absorption measurements were made over the 1.0- to 16-micron range with the sample at room and liquid nitrogen temperatures. The results are similar to those for neutron irradiation and are given in table 2.

DESCRIPTION OF EXPERIMENT

Silicon Crystals

The high-purity silicon referred to herein is float-zone refined "Hyper Pure" silicon. The following is the manufacturer's analysis of this silicon: resistivity, 2,000 to 3,000 ohm-centimeters; oxygen content nondetectable by infrared, estimated to be about 10 parts per billion; major active impurity-boron, with boron content less than 0.17 parts per billion, which is less than 10^{13} atoms per cubic centimeter in silicon; carbon content perhaps a few parts per million. The manufacturer used neutron activation analysis to determine boron content. Hall coefficients measured as a function of temperature

also indicate boron content to be less than 10^{13} atoms per cubic centimeter. Original resistivity and thickness values for each crystal used are listed in table 3. Crystal designations were assigned for the convenience of the experimenters in cataloging specimens.

The silicon crystals used for infrared absorption measurements were polished disks 1 inch in diameter with thicknesses ranging from 1.3 to 4.0 millimeters.

TABLE 3.- SAMPLE DATA

Crystal	Original resistivity, ohm-cm	Thickness, mm
DC-540-13	2700	1.26
DC-540-16	2700	2.51
DC-921-2	3600	1.92
DC-921-5	3600	1.91
DC-921-9	3300	3.88

Apparatus and Procedure

The proton bombardment was done at the Oak Ridge National Laboratory on the 86-inch (22-MeV) cyclotron, operated at its maximum energy. The silicon crystals were cut and polished before being sent to the cyclotron group for irradiation. The first few silicon crystals were mounted on a cooling probe which mechanically held the crystal against a water-cooled aluminum plate. The temperature of the surface of the crystal facing the proton beam was measured with paints of known melting points. The original objective was to keep the crystal temperature below 100°C during bombardment. The first probe, however, did not accomplish this objective, and the crystal temperature went above 400°C . A second probe, which provided direct water cooling of the back side of the crystal, was then used. Measurements showed that the temperature of the silicon crystal in this probe remained less than 93°C . Hereinafter, the first and second probes are referred to as the "hot" probe and the "cool" probe, respectively.

The high temperature of the first few crystals, although unintentional, nevertheless provided the results which are a major part of this report.

The proton input to the crystal was measured with a current integrator. The current integrator measured the total number of protons striking the insulated sample probe and crystal. A graphite collimator was positioned in front of the sample probe and allowed the protons to be incident on the crystal only. Proton beam current to the crystals ranged from 1 microampere to 2 microamperes and beam time from 45 minutes to 8 hours.

The resistivity and absorption measurements were made from 3 to 6 days after bombardment. The crystals were at room temperature during this period.

Infrared absorption measurements were made over the range 1.0 micron to 30 microns by means of two grating spectrophotometers. A Cary model 14 was used for the 1.0- to 2.6-micron range, and a Perkin-Elmer model 421 from 2.5 to 30 microns. The wavelength accuracy of the Perkin-Elmer is ± 0.05 micron at 21 microns. The Perkin-Elmer instrument was purged with dry nitrogen during use. The infrared spectroscopy was performed with the silicon crystals at three temperatures: 300° K, 80° K, and 12° K. The low temperatures were attained with liquid nitrogen and liquid helium in a specially designed optical cryostat. The 1-inch-diameter (2.5-cm-diam) silicon crystals were mounted in a copper sample holder which was in contact with the cryogenic liquid. The optical windows were of cesium iodide, which transmitted 70 percent at 50 microns. Crystal temperature was measured with a carbon resistance thermometer which had been calibrated against a standard germanium resistance thermometer. The temperature was not controlled, and with liquid helium in the cryostat, varied from 10° K to 17° K according to crystal thickness and degree of thermal contact.

The sample resistivity was measured with a four-point probe as explained by Valdes (ref. 25).

Calculations

The output of the infrared spectrophotometers is recorded on charts as percent transmission versus wavelength or wavenumber. The absorption coefficient α is related to the light intensity by

$$I = I_0 \frac{(1 - R)^2 \exp(-\alpha t)}{1 - R^2 \exp(-2\alpha t)} \quad (1)$$

where

- I intensity of the beam after passing through the sample
- I_0 incident beam intensity
- R reflectivity of the sample surface
- t sample thickness

The reflectivity R is taken to be a constant over the wavelength range investigated with a value of 0.30 as determined by Yoshinaga (ref. 26). The transmission T is the ratio of the intensities:

$$T = \frac{I}{I_0} = \frac{(1 - R)^2 \exp(-\alpha t)}{1 - R^2 \exp(-2\alpha t)} \quad (2)$$

Solving equation (2) for α gives

$$\alpha = \log \left[\frac{(1 - R)^2 + \sqrt{(1 - R)^4 + 4T^2R^2}}{2T} \right] t^{-1} \quad (3)$$

If the absorption coefficient is to be plotted as a function of wavelength, the values of α must be calculated for each point. The calculations were made with the aid of a digital computer by using equation (3).

If it is desired to separate the absorption coefficient of the damage centers α_d from the total absorption coefficient α , such as when the damage absorption is close in energy to a lattice or impurity absorption, α_d is given by

$$\alpha_d = \alpha - \alpha_s \quad (4)$$

where α_s is the absorption coefficient of the unirradiated sample as calculated from a preirradiation spectrum.

The concentrations of acceptors in the silicon were determined from the measured values of resistivity according to Conwell (ref. 27). The calculation of acceptor concentrations from absorption coefficients is based on data by Newman (ref. 28). The accuracy of these values is limited because of the nonuniformity of the density of the acceptors in the irradiated silicon. The absorption coefficient perhaps gives the best estimate because the infrared beam effectively integrates over the volume of sample through which it passes. The error in the acceptor concentration is estimated to be ± 30 percent.

RESULTS

Crystal DC-540-13 was mounted on the hot probe and received 2 microamperes of 22-MeV proton current for approximately 45 minutes. The beam was incident on an area of 4.5 centimeters so that an integrated flux of 7.5×10^{15} protons/centimeter² resulted. An absorption spectrum recorded after irradiation showed three new absorption peaks at 18.9, 21.1, and 22.0 microns (fig. 1). The crystal was heated for 3 hours at 600° C. Absorption spectra were made after annealing to determine the effect of annealing on the absorption centers. No change in the magnitude of the three absorption peaks was noted. The minimum resistivity was 330 ohm-centimeters (p-type) on the beam side and 460 ohm-centimeters (p-type) on the back side.

Crystal DC-540-16 was mounted on the hot probe and received a proton beam current of 2 microamperes for approximately 45 minutes over an area of 4.5 centimeters² to obtain an integrated flux of 7.5×10^{15} protons/centimeter². Absorption spectra showed the same three lines with the same magnitude as in crystal DC-540-13. (See

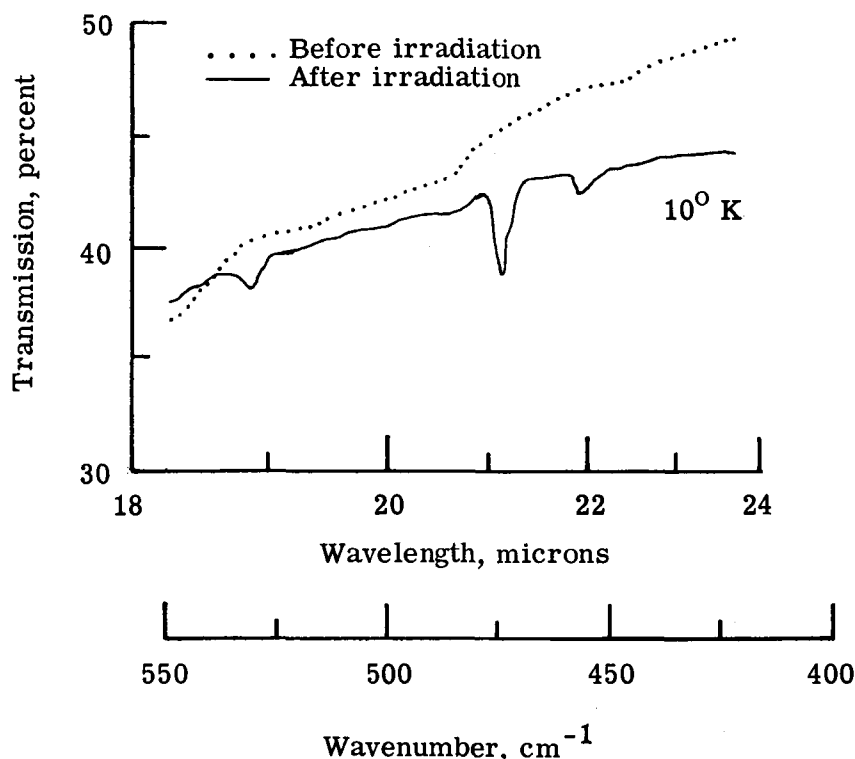


Figure 1.- Absorption spectrum of crystal DC-540-13.
 $\phi = 7.5 \times 10^{15}$ protons/cm²; hot probe.

fig. 2.) Spectra were made with the sample at room temperature, liquid nitrogen temperature, and liquid helium temperature. The absorption lines appeared only at liquid helium temperatures. The resistivity of the crystal was measured at points along a diameter across both faces of the crystal. The results are shown in figure 3. About 0.1 millimeter of material was ground off of each side of the crystal and the faces repolished. Another spectrum was made. There was no decrease in the absorption coefficient of the 19-, 21-, and 22-micron lines. The crystal was annealed at 1000° C for 2 hours. The 19-, 21-, and 22-micron lines disappeared and lines of slightly smaller magnitudes appeared which are identified as being due to substitutional aluminum.

Crystal DC-921-2 was mounted on the hot probe and bombarded for 45 minutes with a 2-microampere proton beam that produced an integrated flux of 7.5×10^{15} protons per centimeter². The absorption spectrum was recorded (fig. 4), and the 18.9-, 21.1-, and 22.0-micron lines were the only new absorptions noted. After bombardment, the lowest resistivity measured on the beam side of the crystal was 70 ohm-centimeters (p-type) and on the back side 150 ohm-centimeters (p-type).

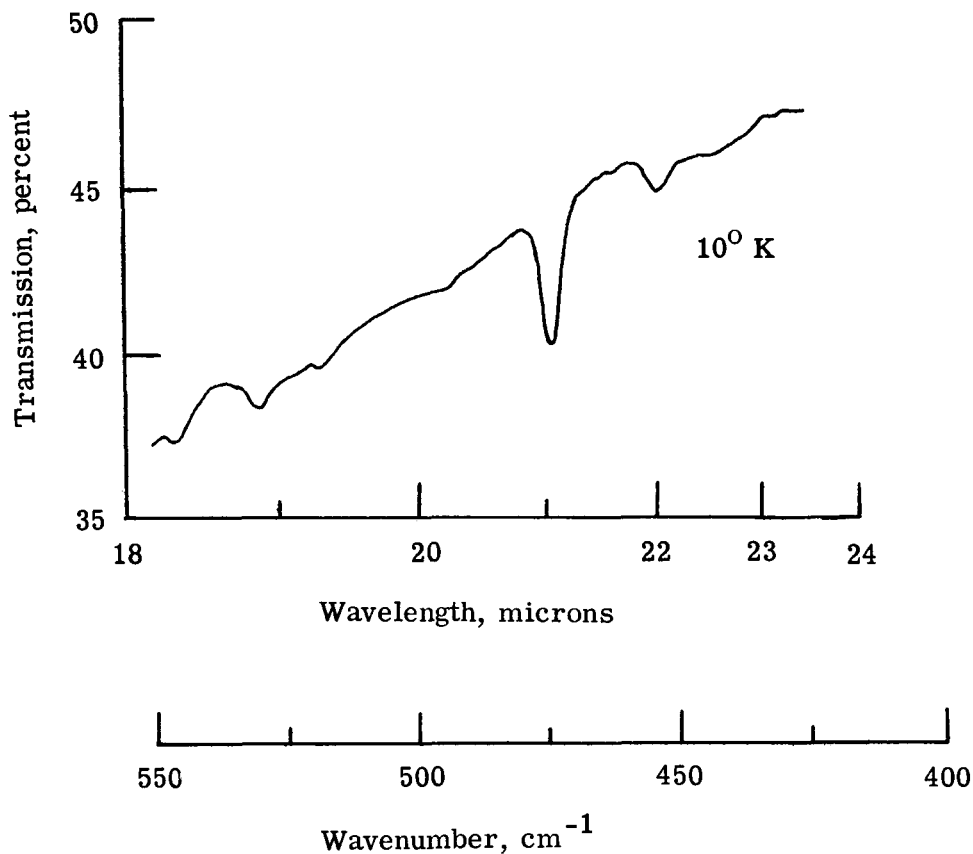


Figure 2.- Absorption spectrum of crystal DC-540-16.
 $\phi = 7.5 \times 10^{15}$ protons/cm²; hot probe.

Crystal DC-921-5 was mounted on the hot probe and received a 2-microampere beam current for 5.8 hours that produced an integrated flux of 5.75×10^{16} protons per centimeter². An absorption spectrum (fig. 5) after bombardment showed the 18.9-, 21.1-, and 22.0-micron lines with increased magnitude plus lines at 19.34 and 22.6 microns which have been identified as aluminum in silicon (ref. 19). A map of the values of resistivity across both sides of the crystal was made (fig. 6). The lowest resistivity measured was 9 ohm-centimeters (p-type) on the beam side and 25 ohm-centimeters (p-type) on the back side.

Crystal DC-921-9 was mounted on the cool probe and received 1-microampere proton beam current for approximately 8 hours over a 2-centimeter² area giving an integrated flux of 9.2×10^{16} protons/centimeter². Resistivity measurements gave 10^5 ohm-centimeters on the beam side and 3×10^4 ohm-centimeters on the back side. The absorption edge had shifted to longer wavelength, and absorption bands were found at 1.8, 3.46, 3.62, 5.5, and 20.5 microns. The crystal was heated for 4.5 hours at 300° C.

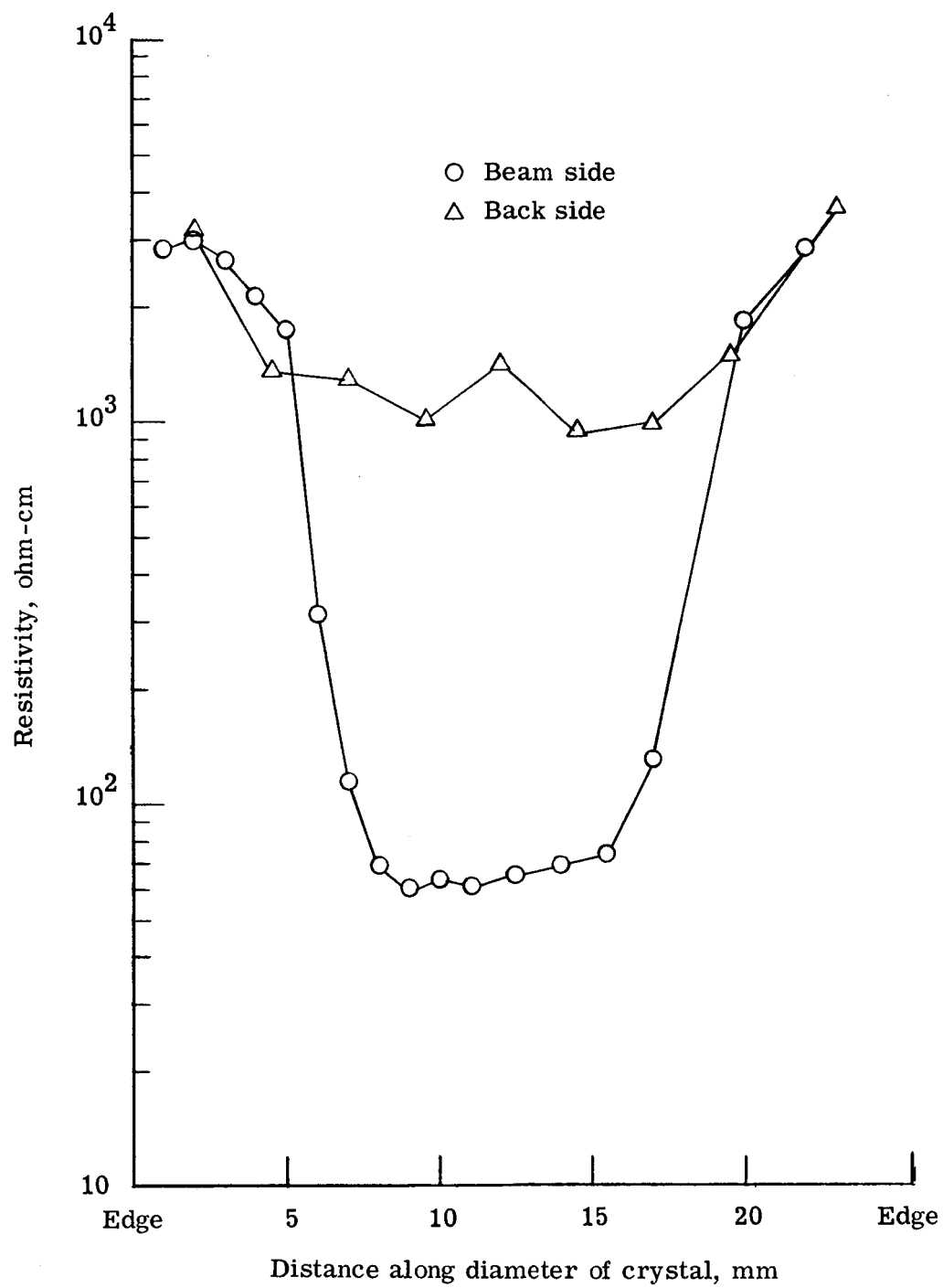


Figure 3.- Resistivity profile of crystal DC-540-16.

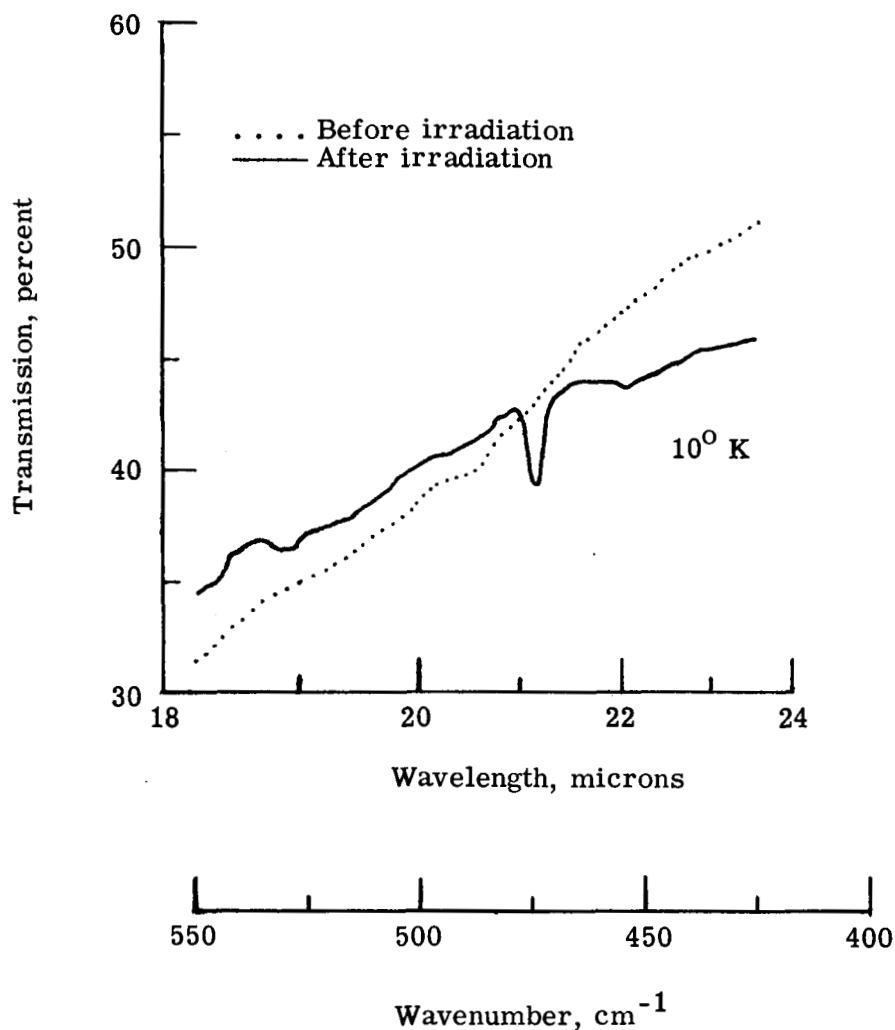


Figure 4.- Absorption spectrum of crystal DC-921-2.

$\phi = 7.5 \times 10^{15}$ protons/cm²; hot probe.

The 1.8-, 3.46-, 3.62-, and 20.5-micron bands annealed out and new bands appeared at 8.9 and 14.2 microns. (See fig. 7.) The crystal was then heated for 7 hours at 600° C. The resistivity decreased to 9 ohm-centimeters (p-type) on the beam side and 8000 ohm-centimeters (p-type) on the back side. The absorption lines at 8.9 and 14.2 microns annealed out, and the absorption spectrum of substitutional aluminum, hereinafter denoted Al_S, appeared (fig. 8). The crystal was heated at 800° C for 2 hours. The resistivity decreased to 3.5 ohm-centimeters on the beam side and increased to 2×10^5 ohm-centimeters on the back side. An absorption spectrum showed growth of the Al_S lines. Heating at 1000° C for 2 hours produced little or no change in the resistivity or Al_S absorption lines.

The treatments received by each crystal and the results of each treatment are listed in table 4.

TABLE 4.- TREATMENT AND RESULTS FOR SILICON CRYSTALS

Crystal	Integrated flux, protons/cm ²	Probe	Annealing temperature, °C	Absorption lines, μ	Minimum resistivity, ohm-cm
DC-540-13	7.5×10^{15}	Hot	{ Unannealed 600	18.9, 21.1, 22.0 18.9, 21.1, 22.0	----- 330
DC-540-16	7.5×10^{15}	Hot	{ Unannealed 1000	18.9, 21.1, 22.0 19.4, 21.2, 22.5	60 -----
DC-921-2	7.5×10^{15}	Hot	Unannealed	18.9, 21.1, 22.0	70
DC-921-5	57.5×10^{15}	Hot	Unannealed	18.9, 21.1, 22.0	9
DC-921-9	92×10^{15}	Cool	{ Unannealed 300 600 800 1000	{ 1.8, 5.5, 3.46, 3.62, 20.5 8.9, 14.2 19.4, 21.2, 22.5 19.4, 21.2, 22.5 19.4, 21.2, 22.5	{ 30 000 ----- 9 3.5 3.5

An activation analysis made on a silicon crystal at the Oak Ridge National Laboratory as soon as possible after bombardment on the cool probe showed the 1.28 Mev γ from the $\text{Al}^{29} \xrightarrow{\gamma, \beta^-} \text{Si}^{29}$ decay. Calculations based on the count rate gave a production rate for Al^{29} of 5.6×10^{-5} atoms/proton. For crystal DC-921-9 this gives a total of 1.0×10^{13} atoms of Al^{29} produced in the crystal by proton bombardment. The half life of Al^{29} is 6.6 minutes.

The concentration and production rates of the acceptors in each crystal were calculated. The results are listed in table 5.

TABLE 5.- ACCEPTOR CONCENTRATIONS AND PRODUCTION RATES

[Accuracy of values is estimated to be ± 30 percent]

Crystal	Concentration, acceptors/cm ³		Production rate, acceptors/proton
	From infrared data	From resistivity	
DC-540-13	4.7×10^{14}	Not measured	8×10^{-3}
DC-540-16	3.2	2.2×10^{14}	11
DC-921-2	3.5	1.9	10
DC-921-5	21	15	7.5
DC-921-9	27	40	6

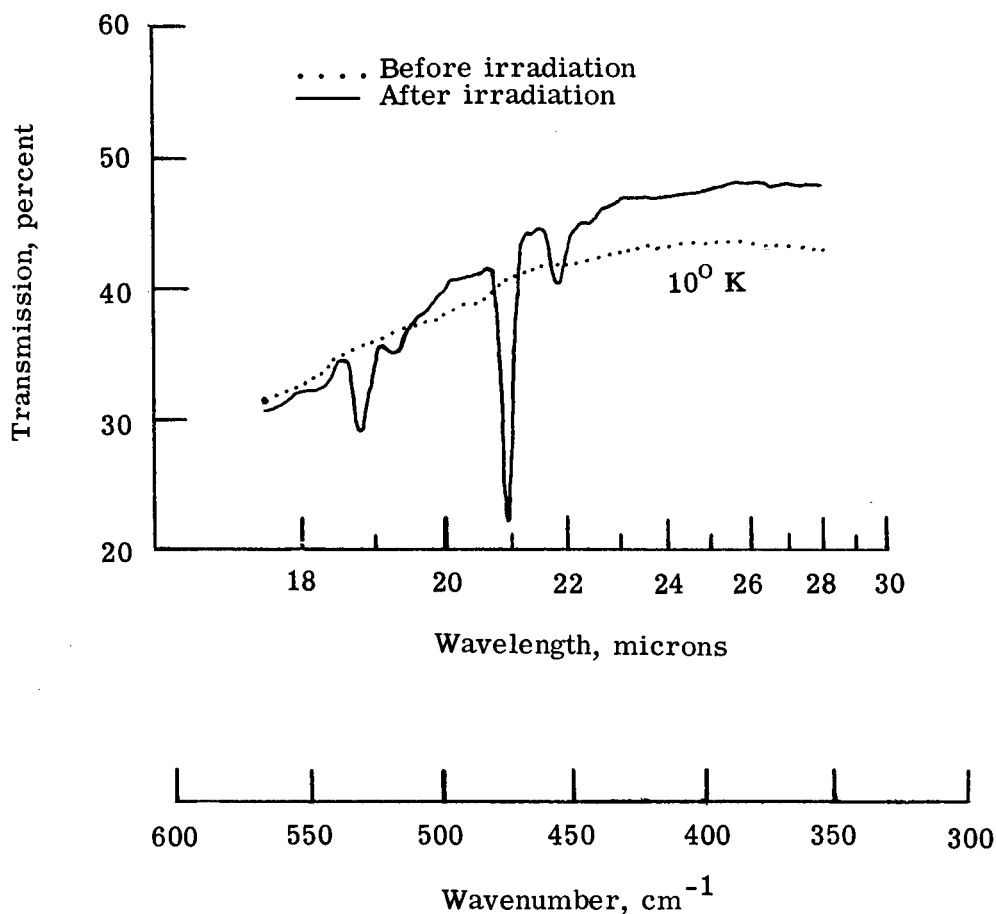


Figure 5.- Absorption spectrum of crystal DC-921-5.
 $\phi = 5.8 \times 10^{16}$ protons/cm²; hot probe.

DISCUSSION

Production of Acceptors

All four silicon samples which were bombarded on the hot probe showed an increase in conductivity, p-type; this result indicates that acceptor states are produced in silicon by proton bombardment. The resistivity of the portions of the crystals which were shielded from the proton beam remained high, as did the resistivity of the back side of those crystals which were thicker than the range of the 22-MeV protons in silicon. The acceptors were produced only in portions of the crystal which were exposed to the proton beam. The beam profile of the cyclotron is known to be nonuniform. This is evidenced

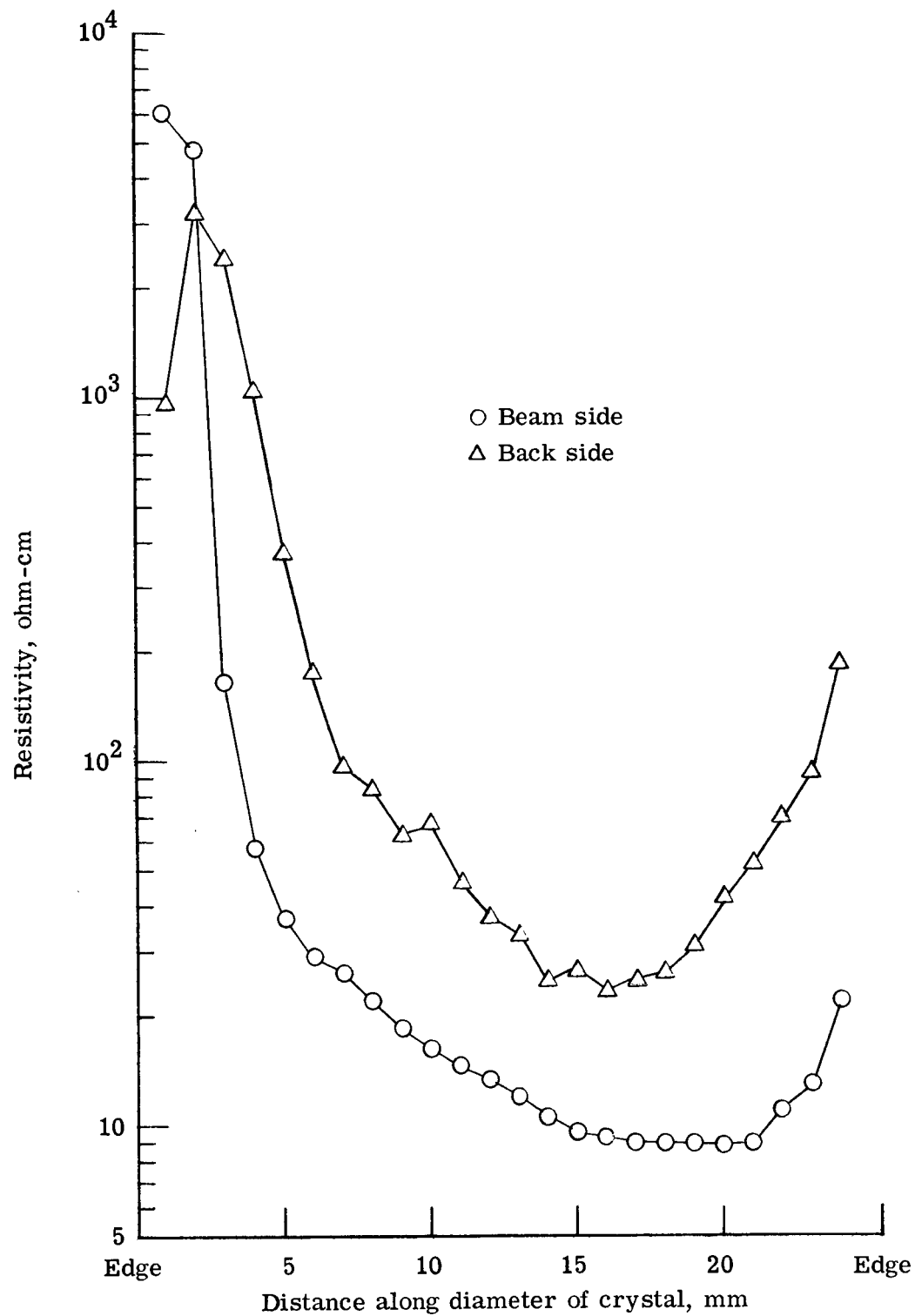


Figure 6.- Resistivity profile of crystal DC-921-5.

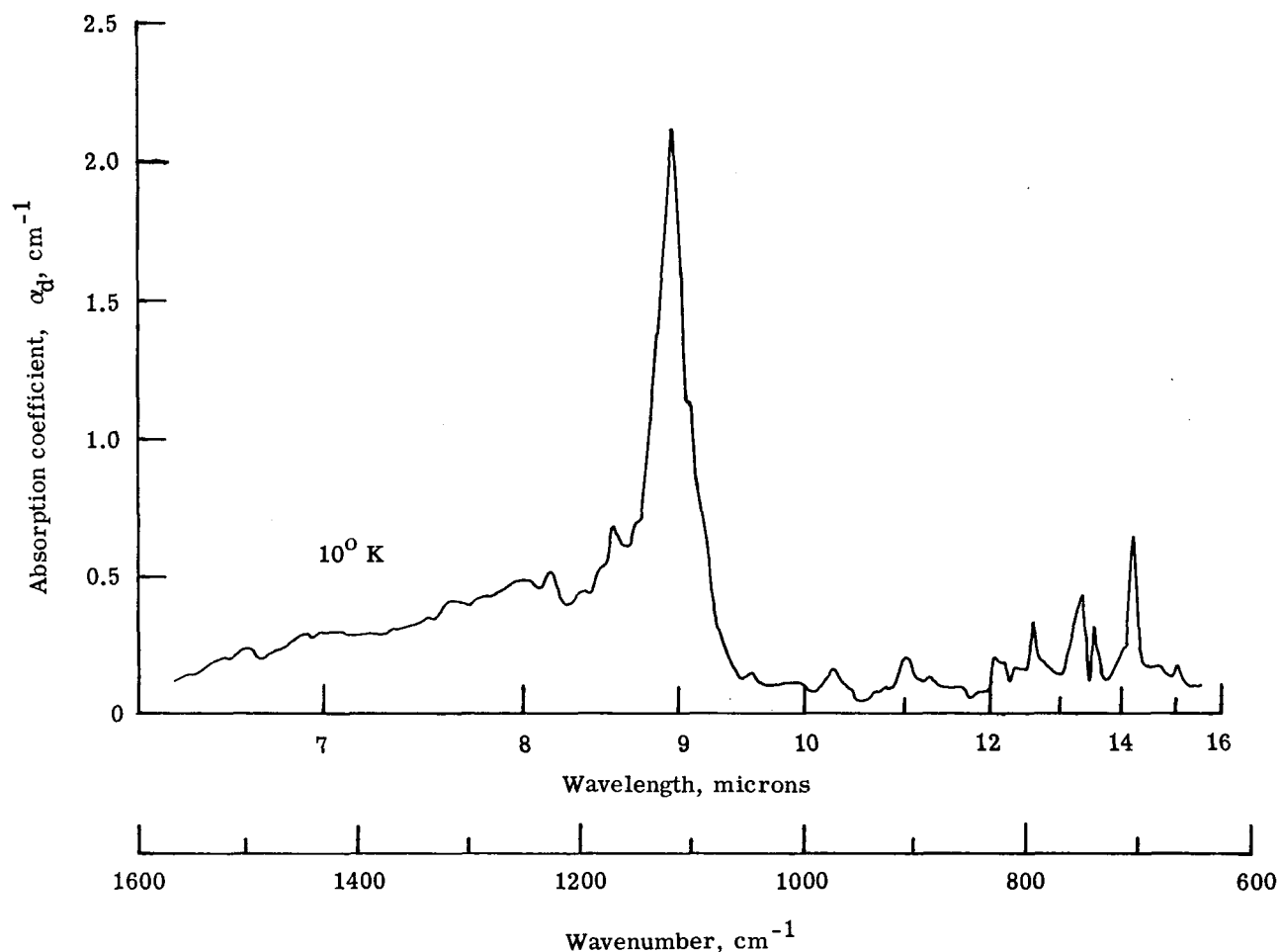


Figure 7.- Absorption spectrum of crystal DC-921-9 after annealing at 300° C.
 $\phi = 9.2 \times 10^{16}$ protons/ cm^2 ; cool probe.

in the resistivity profile of the crystals. The possibility of the acceptors being in-diffused impurities was eliminated because of their location in the crystal.

All absorption spectra of the crystals bombarded on the hot probe showed absorption lines at 18.9, 21.0, and 22.0 microns. These lines have not been previously reported in the literature. They are referred to herein as the "new acceptor" lines for purpose of identification. The new acceptor lines were not observed with the sample at room or liquid nitrogen temperature but were observed only with the sample at liquid helium temperature. This result indicates the absorption to be electronic in nature. The absorption coefficients for these lines were larger in the crystals which received larger proton doses.

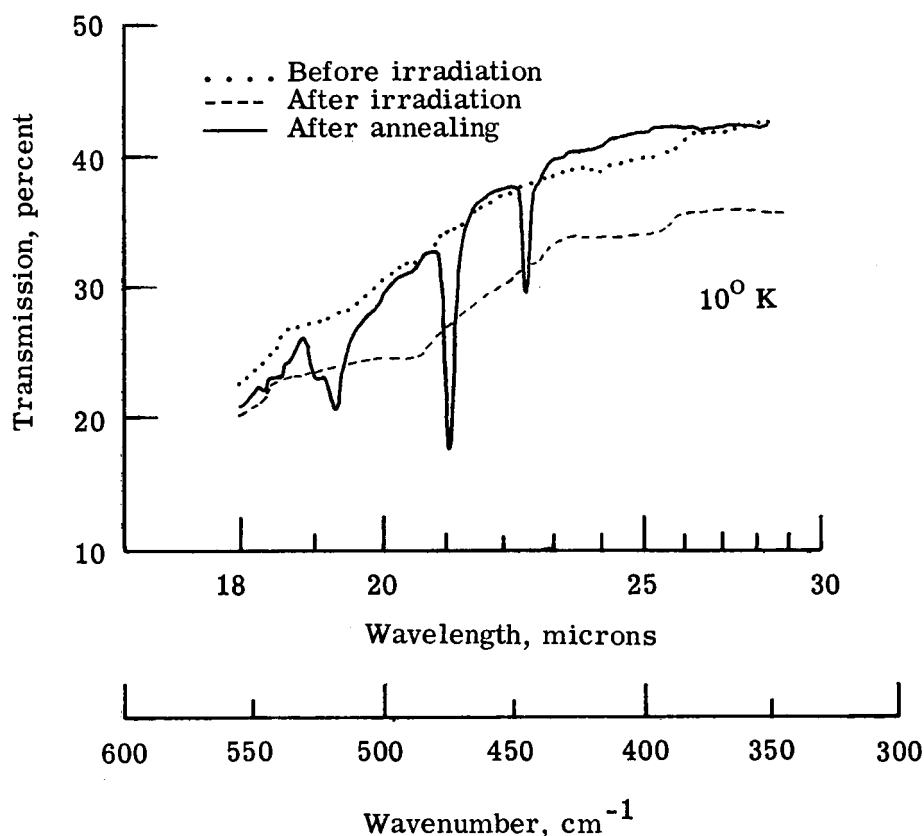


Figure 8.- Absorption spectrum of crystal DC-921-9 after annealing at 800° C. $\phi = 9.2 \times 10^{16}$ protons/cm²; cool probe.

The acceptors responsible for the increased conductivity are concluded to be the centers responsible for the absorption because: (1) both are electronic, (2) both are proportional to the proton dose, and (3) the concentrations of acceptors estimated from resistivity measurements are near those estimated from the absorption coefficients.

The absorption spectrum of the new acceptor lines is very similar in both energy and structure to that of substitutional aluminum, Al_S. Spectra of both are shown in figure 9 for comparison.

The new acceptor lines which were found in the samples bombarded on the hot probe were not found in samples bombarded on the cool probe. The existence of the Al_S spectrum in the annealed cool-probe sample means that the Fermi level had been lowered enough to permit observation of the new acceptor if it were present. High sample temperature during bombardment is evidently necessary to produce the new acceptor. Perhaps quenching of the sample is necessary also.

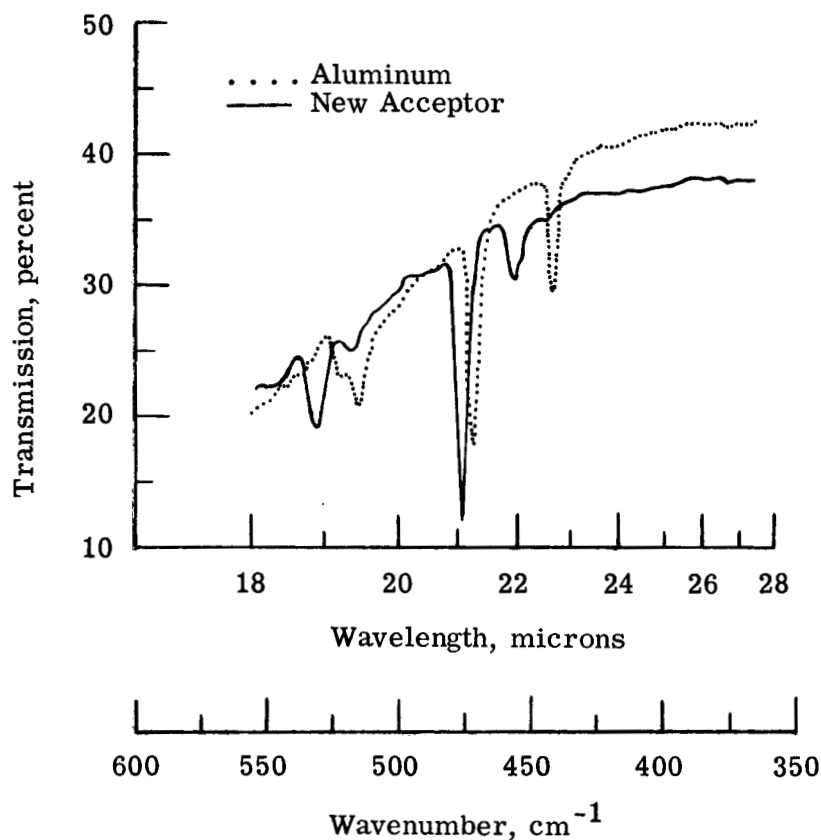


Figure 9.- Comparison of new acceptor and Al_S spectra.

Model for New Acceptor

The positive identification of Al_S in the cool-probe sample, the similarity of the new acceptor and Al_S spectra, and the annealing of the new acceptor into Al_S show the new acceptor to be an aluminum-defect association.

The 18.9-, 21.1-, and 22.0-micron absorption lines of the disturbed aluminum are higher in energy than their corresponding Al_S lines by 2.6 percent, 0.6 percent, and 2.5 percent, respectively.

The next step is to attempt determination of the type of defects in the silicon and the nature of their association with the aluminum atoms. There are two possibilities for the distribution of the defects in the crystal:

Model (a): The defects are distributed randomly throughout the crystal and cause a uniform lattice dilation (ref. 29), which could increase the energy of the excited-hole states by decreasing the dielectric constant or changing the effective mass of the hole.

Model (b): The defects are closely associated with the aluminum atoms causing individual perturbations of the excited hole states.

The close-association model (b) is favored over the random-distribution model (a) for the following reasons:

(1) The Al_S absorption lines which appear together with the new acceptor lines are distinct, and there is no noticeable absorption between the corresponding Al_S and new acceptor lines. This result would require, for the random distribution, a region of uniformly distributed defects as well as a separate region void of defects. This could possibly be explained by the existence of a temperature gradient in the crystal during bombardment and a strong temperature dependence of the defect; however, it casts some doubt on model (a). The separate Al_S lines are more easily explained by model (b) as the existence of some Al_S atoms without associated defects.

(2) It is difficult to explain the difference in the energy shifts of the different states observed in terms of a uniform lattice effect. However, if the defects exist only near the Al_S atoms, then the radial wave functions of the excited hole states could have different amplitudes in the region of the defect so that different perturbations result. Acceptor wave functions are not well enough understood to attempt to use them in determining the size or location of the defect.

The perturbation is exactly the same for all Al_S atoms, as evidenced by the sharpness of the perturbed lines. This implies that the association between defect and aluminum is uniform, that is, the same for each pair.

The possibility of the associated defect being an interstitial silicon atom is not likely because an interstitial would be expected to donate a valence electron to fill the hole and change the charge state of the Al_S such as in the case of $(Al_S^- + Al_i^{++})^+$ association (ref. 24).

If then the defect is a vacancy, is it a single vacancy, a divacancy, or a higher multiple?

Single vacancies are very mobile at low temperatures but remain in the crystal by associating with impurities or with each other to form divacancies or clusters. It is not likely that the attraction between the aluminum atom and the defect would be electronic bonding because the charge state is unchanged and the energy shift is relatively small. The known (single vacancy) + (impurity atom) defects anneal out at 325° C or less. It is believed that the new acceptor is not Al_S + (single vacancy) since the new acceptor remained intact through annealing at 600° C.

The temperature of the crystals during irradiation on the hot probe is known to be above 400° C and was likely less than 1000° C because the new acceptor anneals out at

1000° C. Pfister (ref. 30) has bombarded silicon with protons at high temperatures and concludes that at 800° to 900° C, vacancies precipitate to form vacancy clusters.

The isolated divacancy in silicon anneals out at 250° to 300° C (ref. 31). If the defect associated with aluminum is the divacancy, then it is required that the aluminum atom have sizeable effect on the divacancy to keep it from annealing out at 600° C. EPR studies of the divacancy in silicon have determined that the divacancy has a donor level at $E_v + \sim 0.25$ eV (ref. 32). If this result is correct, and if the divacancy were associated with the aluminum, then the donor electron would fill the $E_v + 0.068$ eV acceptor level of the aluminum, and the (aluminum + defect) acceptor spectrum would not be observed. Observation of the spectrum therefore indicates that the associated defect is not the divacancy.

Whatever the size of the vacancy cluster, it must be uniform, and the relation of the cluster with the aluminum atom must be uniform also because of the sharpness of the new acceptor lines; that is, the Al_s lines were shifted by a definite amount with no broadening of the lines.

Previously reported absorption lines in irradiated silicon were not found in the crystals which were irradiated on the hot probe. However, these lines were not expected because annealing studies have shown that the defects responsible for the lines anneal out at temperatures lower than that of the crystal on the hot probe.

8.9 and 14.2 Micron Absorptions

All the absorption lines that were present in the crystal immediately after irradiation on the cool probe have been found previously. (See table 2.) The increase in resistivity to very high values shows the production of deep-lying donor and acceptor levels which have positioned the Fermi level somewhere close to the center of the band gap. The new acceptor or Al_s absorption lines were not expected because the acceptor states would be occupied by electrons when the Fermi level is at the center of the band gap.

The crystal was heated to anneal out the defect centers and allow the Fermi level to drop below any shallow acceptors. This process would empty the acceptors, and the transition from the valence band to the acceptor would be observed. After annealing at 300° C, the crystal showed new absorption lines at 8.9 and 14.2 microns. The 8.9-micron line broadens but does not disappear when the sample is warmed to room temperature and leads to the belief that the absorption may be vibrational. The 14.2-micron absorption is strong at 10° K, weak at 78° K, and not observed at room temperature. Both the 8.9- and the 14.2-micron lines disappeared during the annealing at 600° C. The disappearance of the 8.9-micron line after the 600° C annealing indicates the annealing out of the defect center. The appearance of the Al_s spectrum indicates a further lowering of

the Fermi level to a position below the ground state of the aluminum caused by annealing of some donor type defect.

Watkins (ref. 24) observed the pairing of substitutional aluminum and interstitial aluminum, $(Al_S^- + Al_i^{++})^+$, in irradiated aluminum-doped silicon. The pairs formed at 200° C and dissociated at 400° C. The similarity in the conditions of production and annealing of the $(Al_S^- + Al_i^{++})^+$ defect and the defects responsible for the 8.9- and 14.2-micron absorption bands suggests that these defects may be identical.

Aluminum Production Rate

The Al^{29} which was detected in the silicon crystal by activation analysis is produced by a $Si^{30}(p,2p)Al^{29}$ reaction. Assuming an identical (p,2p) production rate for Si^{28} gives an estimate of 3.0×10^{14} atoms of Al^{27} produced in crystal DC-921-9 and a production rate of 1.7×10^{-3} atoms/proton. The error in this estimate depends, of course, on the error in the assumption of equal production rates. The production rate of Al^{27} in crystal DC-921-9 based on a measured absorption coefficient is 6×10^{-3} atoms per proton.

CONCLUSIONS

Bombardment of high-purity silicon with 22 MeV protons has produced Al^{27} at a rate of 6×10^{-3} atoms per incident proton in a thick target. The aluminum was identified by the Al_S absorption spectrum. Three new infrared absorption peaks were observed in the irradiated silicon with main peaks at 8.9, 14.2, and 21.0 microns. The 21.0-micron band required high sample temperature during bombardment for production and is identified as (substitutional aluminum) + (vacancy cluster). The 8.9- and 14.2-micron bands appear and disappear with successive annealing. The possibility is mentioned that one or both of these lines might be due to $(Al_S^- + Al_i^{++})^+$.

The production of aluminum in the crystals eliminated the study of damage in impurity-free silicon but, in return, provided for a study of defect interactions with aluminum. The production rate of aluminum is high enough that anyone studying radiation damage by protons should be aware of the presence of the aluminum.

Langley Research Center,
National Aeronautics and Space Administration,
Langley Station, Hampton, Va., January 31, 1967,
124-09-01-04-23.

REFERENCES

1. Vavilov, V. S.: The Interaction of Radiation Defects With Impurities and Other Defects in Semiconductors. 7th International Conference on the Physics of Semiconductors. 3 - Radiation Damage in Semiconductors, Academic Press, c.1965, pp. 115-127.
2. Watkins, G. D.; Corbett, J. W.; and Walker, R. M.: Spin Resonance in Electron Irradiated Silicon. J. Appl. Phys., vol. 30, no. 8, Aug. 1959, pp. 1198-1203.
3. Fan, H. Y.: Radiation Damage in Semiconductors. 7th International Conference on the Physics of Semiconductors. 3 - Radiation Damage in Semiconductors, Academic Press, c.1965, pp. 1-8.
4. Curtis, O. L., Jr.; and Crawford, J. H., Jr.: Arsenic Impurity Defect Interactions in γ -Irradiated Germanium. 7th International Conference on the Physics of Semiconductors. 3 - Radiation Damage in Semiconductors, Academic Press, c.1965, pp. 143-148.
5. Vavilov, V. S.; Vintovkin, S. I.; Lyutovich, A. S.; Plotnikov, A. F.; and Sokolova, A. A.: Radiation Defects in Very Pure Silicon Crystals. Soviet Phys. - Solid State, vol. 7, no. 2, Aug. 1965, pp. 399-402.
6. Brown, W. L.; Augustyniak, W. M.; and Waite, T. R.: Annealing of Radiation Defects in Semiconductors. J. Appl. Phys., vol. 30, no. 8, Aug. 1959, pp. 1258-1268.
7. James, Hubert M.; and Lark-Horovitz, Karl: Localized Electronic States in Bombarded Semiconductors. Z. physik. Chem., vol. 198, 1951, pp. 107-126.
8. Wertheim, G. K.: Energy Levels in Electron-Bombarded Silicon. Phys. Rev., Second ser., vol. 105, no. 6, Mar. 15, 1957, pp. 1730-1735.
9. Wertheim, G. K.: Electron-Bombardment Damage in Silicon. Phys. Rev., Second ser., vol. 110, no. 6, June 15, 1958, pp. 1272-1279.
10. Spitzer, W. G.; and Fan, H. Y.: Effect of Neutron Irradiation on Infrared Absorption in Silicon. Phys. Rev. (Letters to Ed.), Second ser., vol. 109, no. 3, Feb. 1, 1958, pp. 1011-1012.
11. Ramdas, A. K.; and Fan, H. Y.: Infrared Absorption Spectra of Defects in Irradiated Silicon. J. Phys. Soc. Japan, vol. 18, Suppl. II, Mar. 1963, pp. 33-36.
12. Bemski, G.: Paramagnetic Resonance in Electron Irradiated Silicon. J. Appl. Phys., vol. 30, no. 8, Aug. 1959, pp. 1195-1198.
13. Watkins, G. D.; and Corbett, J. W.: Defects in Irradiated Silicon. I. Electron Spin Resonance of the Si-A Center. Phys. Rev., Second ser., vol. 121, no. 4, Feb. 15, 1961, pp. 1001-1014.

14. Fan, H. Y.; and Ramdas, A. K.: Infrared Absorption and Photoconductivity in Irradiated Silicon. *J. Appl. Phys.*, vol. 30, no. 8, Aug. 1959, pp. 1127-1134.
15. Hill, D. E.: Electron Bombardment of Silicon. *Phys. Rev.*, Second ser., vol. 114, no. 6, June 15, 1959, pp. 1414-1420.
16. Vitovskii, N. A.; Lukirskii, D. P.; Mashovets, T. V.; and Myakota, V. I.: Energy Spectrum of Defects Produced in Silicon by Irradiation With Electrons. *Soviet Phys. - Solid State*, vol. 4, no. 5, Nov. 1962, pp. 840-844.
17. Carter, J. R.; and Downing, R. G.: Charged Particle Radiation Damage in Semiconductors, VII: Energy Levels of Defect Centers in Electron and Proton Bombarded Silicon. MR-30 (Contract NAS 5-1851) Space Technology Labs., Inc., Feb. 15, 1963.
18. Klein, C. A.; and Straub, W. D.: On the Energy Levels in Neutron Irradiated p-Type Silicon. *Bull. Am. Phys. Soc.*, ser. II, vol. 3, no. 7, Nov. 28, 1958, p. 375.
19. Longo, T. A.; and Lark-Horovitz, K.: Irradiation of Silicon With 9.6 Mev Deuterons. *Bull. Am. Phys. Soc.*, ser. II, vol. 2, no. 3, Mar. 1957, p. 157.
20. Becker, M.; Fan, H. Y.; and Lark-Horovitz, K.: Infrared Absorption of Nucleon-Bombarded Silicon. I. *Phys. Rev.*, vol. 85, 1952, p. 730.
21. Corbett, J. W.; Watkins, G. D.; Chrenko, R. M.; and McDonald, R. S.: Defects in Irradiated Silicon. II. Infrared Absorption of the Si-A Center. *Phys. Rev.*, Second ser., vol. 121, no. 4, Feb. 15, 1961, pp. 1015-1022.
22. Corelli, John C.: Radiation Damage to Semiconductors by High-Energy Electron and Proton Radiation. Progress Rept. 15 Sept. 1964 to 15 March 1965. (NASA Grant NsG-290), Rensselaer Polytech. Inst.
23. Blount, E. I.: Energy Levels in Irradiated Germanium. *J. Appl. Phys.*, vol. 30, no. 8, Aug. 1959, pp. 1218-1221.
24. Watkins, G. D.: A Review of EPR Studies in Irradiated Silicon. 7th International Conference on the Physics of Semiconductors. 3 - Radiation Damage in Semiconductors, Academic Press, c.1965, pp. 97-111.
25. Valdes, L. B.: Resistivity Measurements on Germanium for Transistors. *Proc. IRE*, vol. 42, no. 2, Feb. 1954, pp. 420-427.
26. Yoshinaga, Hiroshi: Reflectivity of Several Crystals in the Far Infrared Region Between 20 and 200 Microns. *Phys. Rev. (Letters to Ed.)*, Second ser., vol. 100, no. 2, Oct. 15, 1955, pp. 753-754.
27. Conwell, E. M.: Properties of Silicon and Germanium: II. *Proc. IRE*, vol. 46, no. 6, June 1958, pp. 1281-1300.

28. Newman, Roger: Concentration Effects on the Line Spectra of Bound Holes in Silicon. Phys. Rev., Second ser., vol. 103, no. 1, July 1, 1956, pp. 103-106.
29. Simmons, R. O.; and Balluffi, R. W.: X-Ray and Expansion Effects Produced by Imperfections in Solids: Deuteron-Irradiated Germanium. J. Appl. Phys., vol. 30, no. 8, Aug. 1959, pp. 1249-1258.
30. Pfister, J. C.: Radiation Enhanced Diffusion in Silicon. 7th International Conference on the Physics of Semiconductors. 3 - Radiation Damage in Semiconductors, Academic Press, c.1965, pp. 281-285.
31. Corelli, John C.: Radiation Damage in Semiconductors by High-Energy Electron and Proton Radiation. Progress Rept. 15 Sept. 1965 to 15 March, 1966. (NASA Grant NsG-290), Rensselaer Polytech. Inst.
32. Watkins, G. D.; and Corbett, J. W.: Defects in Irradiated Silicon: Electron Paramagnetic Resonance of the Divacancy. Phys. Rev., Second ser., vol. 138, no. 2A, Apr. 19, 1965, pp. A543-A555.